Fluorescence-guided hepatobiliary surgery with long and short wavelength fluorophores

Thinzar M. Lwin[1], Robert M. Hoffman[1,2,3], Michael Bouvet[1,3]

[1]Department of Surgery, University of California San Diego, San Diego, CA, USA; [2]AntiCancer, Inc., San Diego, CA, USA; [3]VA San Diego Healthcare System, San Diego, CA, USA

Contributions: (I) Conception and design: All authors; (II) Administrative support: None; (III) Provision of study material or patients: None; (IV) Collection and assembly of data: TM Lwin; (V) Data analysis and interpretation: All authors; (VI) Manuscript writing: All authors; (VII) Final approval of manuscript: All authors.

Correspondence to: Michael Bouvet, MD. Department of Surgery, University of California San Diego, Moores Cancer Center, 3855 Health Sciences Drive #0987, La Jolla, CA 92093-0987, USA. Email: mbouvet@ucsd.edu.

Importance: Fluorescence-guided surgery (FGS) is a potentially powerful tool for hepatobiliary (HPB) surgery. The high sensitivity of fluorescence navigation is especially useful in settings where tactile feedback is limited.

Objective: The present narrative review evaluates literature on the use of FDA-approved fluorophores such as methylene blue (MB), 5-aminolevulinic acid (5-ALA), and indocyanine green (ICG) for clinical intra-operative image-guidance during HPB surgery.

Evidence Review: Approaches such as dosing, timing, imaging devices and comparative endpoints are summarized. The feasibility and safety of fluorophores in visualizing the biliary tree, identify biliary leaks, outline anatomic hepatic segments, identify tumors, and evaluate perfusion and graft function in liver transplants are discussed.

Findings: Tumor-specific probes are a promising advancement in FGS with a greater degree of specificity. The current status of tumor-specific probes being evaluated in clinical trials are summarized.

Conclusions and Relevance for Reviews: Relevant discussion of promising tumor-specific probes in pre-clinical development are discussed. Fluorescence-guidance in HPB surgery is relatively new, but current literature shows that the dyes are reliably able to outline desired structures with a variety of dosing, timing, and imaging devices to provide real-time intra-operative anatomic information to surgeons. Development of tumor-specific probes will further advance the field of HPB surgery especially during oncologic resections.

Keywords: Fluorescence-guided surgery (FGS); methylene blue (MB); 5-aminolevulinic acid (5-ALA); indocyanine green (ICG); hepatobiliary surgery (HPB surgery); tumor-specific probes; near-infrared fluorescence (NIR fluorescence)

Introduction

A critical issue in surgical treatment of hepatobiliary (HPB) lesions is the need for accurate localization, resection, and reconstruction, while sparing parenchyma and preserving function. High-resolution, contrast-enhanced pre-operative imaging can approximate the lesion in relation to adjacent structures. However, these images are usually obtained weeks, or even months prior to surgery. Registration of these images with intra-operative anatomy can be imprecise. Once in the operating room, surgeons must rely on visual inspection, tactile palpation and clinical judgment to determine location and set resection margins.

The use of ultrasound and its incorporation into the intra-

operative environment in the 1980's enhanced the precision of tumor localization (1). This gave surgeons the ability to visualize tumors in real-time. The use of intra-operative ultrasound (IOUS) improved the detection and localization of lesions by up to 35% when compared with traditional cross-sectional imaging (2). This is especially useful for lesions not readily visible on the surface of the liver.

Fluorescence imaging can further enhance the ability of surgeons to see lesions in real-time. Fluorescence is based on the use of an exogenous chromophore agent, which emits a signal when excited with light of a specific wavelength. Fluorophores within the visible spectrum emit a signal that is detectable with the naked eye while fluorophores at the near-infrared (NIR) spectrum require an imaging device to detect the signal (3). NIR fluorophores are more commonly used for intra-operative imaging due to decreased light scattering, auto-fluorescence, tissue absorption and increased tissue penetration (4,5). Differential biodistribution of these agents are exploited for contrast enhancement of the surgical field.

The three commonly used, FDA-approved fluorophores for intra-operative imaging are: methylene blue (MB), 5-aminolevulinic acid (5-ALA), and indocyanine green (ICG). The present literature review seeks to describe the clinical uses of these fluorophores in HPB surgery and highlight key relevant studies regarding efficacy. MB is both a visible wavelength non-specific fluorophore when used at millimolar doses and an NIR 700 nm fluorophore when used at micromolar doses. 5-ALA is visible wavelength semi-specific fluorophore. Both MB and 5-ALA have been used to a limited degree for fluorescence-guided HPB surgery and therefore will only be briefly discussed here. ICG is a non-specific NIR fluorophore and has a rapidly-expanding body of literature describing its applications for intra-operative guidance of HPB procedures. The use of ICG for visualizing the gallbladder, bile ducts, liver segments, liver tumors, and liver transplant will be discussed. While ICG as a NIR fluorophore is sensitive, it is not specific and tumor-specific fluorescent antibodies are an exciting next generation of probes. Currently, developing molecules and their status in clinical trials will also be reviewed here.

We present the following article in accordance with the Narrative Review reporting checklist (available at http://dx.doi.org/10.21037/hbsn.2019.09.13).

Methods

A Medline search was performed via PubMed using the keyword "fluorescence" with the following HBP surgery related keywords: "cholecystectomy", "cholangiography", "bile duct", "hepatectomy", "hepatic resection", "liver resection", "hepatobiliary surgery", "liver transplant", "pancreatic surgery" in conjunction with the following 3 fluorophores "methylene blue", "5-ALA", "ICG". Studies on the use of fluorescence-guided surgery (FGS) for pancreatic surgery were deferred for the purpose of this manuscript. Original studies were retrieved and selected by authors for clinical relevance to FGS. Papers were selected for their use of fluorophores for clinical intra-operative image-guidance during HPB surgery. Approaches and uses of the fluorophores are summarized. Studies were required to be written in English, and accessible through the University of California Systems Library. Pre-clinical animal studies and reviews were not included here. Studies were organized into a database using Microsoft Excel and summarized into tables. In discussing tumor-specific NIR fluorescent probes, relevant pre-clinical studies are mentioned. To evaluate current status of FGS in clinical trials, a review of clinicaltrials.gov was performed using the following HPB surgery related key words with fluorescence related keywords such as "ICG", "fluorescence", "fluorescence-guided surgery", "fluorophore", and "near-infrared as well as "tumor-specific probes". Additional searches were performed directly using the names of the principal investigators resulted on the initial query. References of the included articles were checked to ensure that no additional relevant studies were missed with the search criteria. The number of overall articles recovered and reviewed specific to each topic are summarized in *Table 1*.

MB

MB is a water soluble heptically and renally eliminated molecule which traditionally has been used at high millimolar doses for sentinel lymph node detection under bright light in melanoma and breast cancer (6). At low micromolar concentrations, it exhibits fluorescence properties, emitting a peak signal at 688 nm (7). The mechanism behind the accumulation of MB at tumors is unclear. Within the field of HPB surgery, MB has been used more commonly as a visible stain with white-light visualization rather than as a fluorophore for FGS. It has been used to delineate anatomic segments, check for bile leaks, and evaluate extrahepatic biliary structures. When using MB as a contrast agent during cholecystectomy, the dye is injected directly into the gallbladder infundibulum

Table 1 Summary of number of articles reviewed for relevance to FGS

Variable	Studies identified	Relevant studies
MB		
Cholecystectomy	1	1
Cholangiography	1	1
Bile duct	3	2
Hepatectomy	2	0
Hepatic resection	1	1
Liver resection	5	2
Liver surgery	4	2
Hepatobiliary surgery	1	0
Liver transplant	0	0
5-ALA		
Cholecystectomy	0	0
Cholangiography	0	0
Bile duct	1	0
Hepatectomy	3	3
Hepatic resection	4	3
Liver resection	11	4
Hepatobiliary surgery	0	0
Liver surgery	26	5
Liver transplant	6	0
ICG		
Cholecystectomy	39	33
Cholangiography	44	33
Bile duct	60	2
Hepatectomy	51	28
Hepatic resection	35	21
Liver resection	87	33
Hepatobiliary surgery	40	5
Liver surgery	130	33
Liver transplant	31	14

MB, methylene blue; 5-ALA, 5-aminolevulinic acid; ICG, indocyanine green.

to outline the extrahepatic biliary tree (8). During liver surgery, MB can be directed to the segment to be removed via injection of dye into the appropriate portal vein branch under ultrasound guidance (9). MB was found to be most useful during parenchymal dissection as there was a clear color difference between the two areas beyond surface boundaries (10). When used to detect bile leaks at the cut edge of the liver, the dye is injected through a trans-cystic tube. In several studies, the postoperative biliary leakage rate was reduced by the MB test (3.6% *vs*. 7.3%, P<0.05) and on multivariate analysis, the absence of an MB test was an independent risk factor for a bile leak (OR =2.6, 95% CI: 1.43–4.65, P=0.002) (11,12). In transplant surgery, it was used to demonstrate that abdominal drains were not needed after donor hepatectomies if the MB bile leak test was negative (13).

MB has more commonly been used as a visible dye under white light for HPB procedures, but due to the superior tissue penetration of NIR fluorescence and its ability to emit a signal at around 700 nm, it has recently been explored as an agent for FGS. While there is limited use of MB for FGS described in the clinical literature, it has been compared against ICG in some pre-clinical studies and the advantages of a low liver signal, rapid fluorescence (within 5–20 minutes), and possibility of repeat dosing were noted (14,15). The disadvantages are that the signal overall is weaker and the mechanism by which MB accumulates at lesions is unclear. The dye also has the potential adverse effects of interfering with pulse oximetry, skin or urine discoloration, and anaphylaxis and hemolysis in G6PD-deficient patients.

As a fluorophore for fluorescence-guided HPB procedures, MB has only been examined in isolated case reports. There were no studies evaluating the use of MB in fluorescence-guided hepatectomies, cholecystectomies, or in liver transplants.

5-ALA

5-ALA is a water-soluble molecule that is processed by the porphyrin synthesis pathway into protoporphyrin IX (PPIX) that emits a peak signal at 635 nm (16). PPIX in normal cells is converted to heme by ferrochelatase (FC) in mitochondria

and eventually excreted into bile after heme is converted to biliverdin and bilirubin in the cytoplasm. The fluorophore is semi-selective. The fluorescence signal in cancer cells is due to increased porphobilinogen deaminase (PBG-D) synthesis of PPIX and decreased activity of FC, leading to an overall preferential accumulation of PPIX at tumors (17). 5-ALA can penetrate the blood-brain barrier and this property has been exploited for FGS of brain tumors (18). It has also been utilized in dermatology and urology for detection of lesions (19,20).

Regarding HPB procedures, 5-ALA has been evaluated for visualization of liver lesions. There are 5 studies describing the use of 5-ALA for visualization in the literature. Schneider *et al.* first described fluorescence intra-operative imaging of hepatocellular carcinoma (HCC) (described as "photodynamic diagnosis" or PDD) in a case report of a patient with HCC who was found to have additional hepatic micro-metastases which would have been missed with conventional white-light laparoscopy (21). In this case report, they used an oral solution of 20 mg/kg 5-ALA and imaged with the Storz D-Light AF-system laparoscope (Karl Storz GmbH, Tuttlingen, Germany) 6 hours after administration. In their subsequent case series they reported that the use of fluorescence imaging yielded detection of more metastatic lesions in 4 of 9 patients compared to white light (22). While the work demonstrated the feasibility of detection, it did not describe the surgical resection based on fluorescence-guidance.

Work by Inoue *et al.* describes the largest experience with 5-ALA-based FGS. The group first described their experience with a series of 70 patients who underwent liver resection for liver tumors (23). The patients had oral administration of 1 gram of 5-ALA in 20 mL 50% glucose solution 3 hours prior to surgery and imaging was performed with a specific blue light (Esperaluz ESLZ-PD-HLVL405; CCS Inc., Kyoto, Japan) and a SC-52 Fuji filter (Fuji Film, Tokyo, Japan) for open surgeries and a Storz D-Light AF-laparoscope (Karl Storz GmbH, Tuttlingen, Germany) for minimally-invasive procedures. They note that the technology was most useful for tumors on the surface of the liver and was especially useful in laparoscopic surgery where palpation is limited. It was effective for margin assessment during parenchymal transection. There was a100% sensitivity for detection of HCC, 85.7% for colorectal liver metastases (CLM), and 100% for liver tumors of various etiologies with an overall sensitivity of 5-ALA for detection of 92.5%. The margins of resection were negative for all patients in the case series (*vs.* 8%

in their historical controls) despite having significantly smaller margin width in the specimen of 6.7±6.9 (range 0–27) mm [*vs.* 9.2±7.0 (range 0–47) mm in their historical controls] (P=0.0083) that was attributable to fluorescence guidance. The same group compared the use of 5-ALA and ICG in 134 patients using 5-ALA, 1 gram given 3 hours before surgery with imaging devices as described above, and 0.5 mg/kg of ICG intravenously 14 days after surgery using photodynamic eye (PDE) (Hamamatsu Photonics, Shizuoka, Japan) for imaging. The sensitivity, specificity and accuracy of 5-ALA for detecting the main tumors were 57%, 100% and 58%, respectively, compared to the sensitivity, specificity and accuracy of ICG of 96%, 50% and 94% respectively. The use of fluorescence technology allowed detection of 5 additional lesions missed by pre-operative imaging. They noted that ICG was more sensitive and less specific while 5-ALA was more specific but less sensitive, but both were useful in detecting small superficial tumors on the liver surface.

Inoue *et al.* also retrospectively evaluated the use of 5-ALA PDD for visualization of bile leaks in the above cohort of patients (24). As the metabolized product is extracted in the bile, it is detectable by fluorescence. Rather than retrograde injection of various dyes at non-physiologic pressures, the physiologic metabolism and biliary excretion after oral 5-ALA intake make it useful for detection of bile leaks at physiologic draining pressures without the use of catheters to cannulate the biliary tree. There were 9 patients with intra-operatively detected bile leaks, but the use of fluorescence imaging with 5-ALA showed a bile leak in 6 additional patients. They concluded that there was a statistically-significant difference although they number of patients who had bile leaks diagnosed using 5-ALA fluorescence imaging was very small.

5-ALA is a useful, orally-administered compound for intra-operative fluorescence imaging and guidance of liver lesions and bile leaks. It has not been described for use in fluorescence-guided cholecystectomy or liver transplant. 5-ALA is a semi-selective fluorophore for tumors based on their aberrant metabolism of the dye. It is more specific than either MB or ICG based on the limited literature available. It has limited signal in the hepatic parenchyma, but is more concentrated in bile, making it potentially useful to evaluate bile leaks. Drawbacks are that it is a visible wavelength fluorophore and is very limited in visualizing deeper lesions, an issue commonly described in the studies mentioned above. While minor, its route of oral administration can be an issue in patients who are

unable to tolerate any oral intake. Additionally, it appears to cause adverse reactions such as photodermatosis (sunburn) needing 24 hour avoidance of sunlight exposure, GI upset, and abnormalities in liver function tests (25,26).

ICG

ICG is a water-soluble molecule that binds to plasma proteins, undergoes hepatic metabolism and biliary elimination (27). It was initially used for fundoscopy and estimation of cardiac and hepatic function (28). However due to its vascular partitioning, near exclusive biliary elimination mechanisms, and low toxicity, it has been used for a number of surgical procedures. ICG emits at NIR wavelengths with a peak signal at 830 nm that allows for increased tissue depth penetration of up to 10 mm (29). There are a wide array of ICG-optimized surgical imaging devices available (5,30). The NIR wavelength window also has decreased auto-fluorescence leading to background noise and increased contrast of the visualized structure (4). ICG has been widely used to evaluate tissue perfusion and lymphatic mapping. Within the field of HPB surgery, the hepatic metabolism of ICG makes it useful for many intra-operative real-time imaging approaches. It is especially useful for non-invasive fluorescence cholangiography to evaluate the biliary tree. It can be used to selectively perfuse segments of the liver to better identify the boundaries of anatomic resection as well as to detect bile leakage after hepatic resections. Due to the enhanced permeability and retention (EPR) of ICG by disorganized neoplastic tissue, it is also useful in oncologic procedures, especially visualizing cancers of the HPB system.

ICG for evaluating the gallbladder and biliary tree

Intra-operative cholangiography (IOC) has been essential for intra-operative visualization of the biliary tree since its first introduction in 1930's by Dr. Mirizzi (31). The use of IOC allows surgeons to better define the biliary anatomy, achieve early recognition and decrease severity of biliary injury should it occur (32). However, IOC is often cumbersome, resource-intensive, requires X-ray exposure, and administration of contrast which is invasive as it requires cannulation of the biliary tree. There can also be anatomic limitations to IOC especially in the setting of severe cholecystitis with friable tissue leading to inability to cannulate and further dissection would lead to increased risk of biliary injury.

Ishizawa first showed feasibility of ICG cholangiography to evaluate the biliary system by comparing trans-cystic administration and intravenous administration of ICG in 2008 using an open-field NIR fluorescence imaging device in patients undergoing open donor hepatectomy or open cholecystectomy (33). This approach was adapted into a minimally-invasive setting using intravenous ICG administration with a fluorescence laparoscope for patients undergoing laparoscopic cholecystectomy. In all 52 patients, the cystic duct was easily identified, and in 50 patients the cystic to common hepatic duct junction was easily identified under fluorescence prior to any dissection (34). After dissection, the cystic to common hepatic duct junction was identified in all patients under fluorescence imaging. The technology also identified unusual biliary anatomy such as accessory hepatic ducts and unusual cystic to common hepatic duct junctions, such as short cystic ducts and parallel or spiral junctions which place patients at high risk of bile duct injuries.

There were 33 different studies from different groups reporting on the results of their studies of cholecystectomies under fluoresence guidance. They are summarized in *Table 2*. Fluorescence-guidance is useful in helping identify the cystic duct-common bile duct (CD-CBD) junction during cholecystectomies for many indications: cholelithiasis, acute cholecystitis, chronic cholecystitis, or cholecystitis needing a percutaneous cholecystostomy tube. Optimal dosing of ICG and timing of visualization are still variable, as demonstrated in *Table 2*, a dose of 2.5 mg intravenous approximately 1–2 hours prior to surgery seems to be the most widely used approach with acceptable liver background fluorescence. There is variability in approaches to dye delivery: intravenous *vs*. direct biliary injection. Regardless of the dose, schedule and route, the use of ICG was effective in identifying the critical view of safety (CVS) during different approaches to cholecystectomies in the reviewed studies. These groups looked at laparoscopic, robotic, or single-incision approaches to fluorescence-guided cholecystectomies using a variety of fluorescence-enabled scopes. Hammamatsu, Storz, Stryker, Noavadaq, Olympus, and DaVinci Flirefly are the most commonly used in the operating room. The strength of the light source, the sensitivity of the camera capturing images, the proprietary software to process the image and render a "threshold" to display a positive fluorescence signal, as well as the final image output format (black and white *vs*. color overlay *vs*. intensity-based heat map) are heterogeneous and variable across different devices. All these above factors affect the

Table 2 Summary of studies using ICG for cholecystectomy

Author	Year	n	Study design	Surgery	ICG dose	Timing	Fluorescence imaging system	IR of CD (%)	IR of CBD/ CHD (%)	Complications of dye injection	Post-operative outcomes
Mitsuhashi et al. (35)	2008	5	Case series	Open	2.5 mg	30 min before surgery	Hammamatsu	100% (5/5)	100% (5/5)	None	No post-operative adverse events
Ishizawa et al. (33)	2009	10	Case series	Open	2.5 mg	60 min before surgery/during conversion to open	Hammamatsu	90% (9/10)	90% (9/10)	None	Not reported
Aoki et al. (36)	2010	14	Case series	Laparoscopic	12.5 mg	30 min before surgery	Hammamatsu	71% (10/14)	71% (10/14)	None	Not reported
Tagaya et al. (37)	2010	12	Case series	Open (n=4), laparoscopic (n=8)	2.5 mg	60–120 min before surgery	Experimental scope/ Hammamatsu	100% (12/12)	100% (12/12)	None	Not reported
Ishizawa et al. (34)	2010	52	Case series	Laparoscopic	2.5 mg	30 min before surgery	Hammamatsu	100% (52/52)	96% (50/52)	None	No post-operative adverse events
Ishizawa et al. (38)	2011	7	Case series	SILS	2.5 mg	After intubation	Hammamatsu	100% (7/7)	100% (7/7)	None	No post-operative adverse events
Buchs et al. (39)	2012	12	Case series	SIRS	2.5 mg	45 min before surgery	Intuitiv	100% (12/12)	83.3% (10/12)	None	No post-operative adverse events
Kaneko et al. (40)	2012	28	Case series	Laparoscopic, SILS	2.5 mg	15 min before surgery/during surgery	Hammamatsu	93% (26/28)	96% (27/28)	Not reported	Not reported
Buchs et al. (41)	2013	23	Comparative case series	SIRS	2.5 mg	After intubation	DaVinci	Not reported	Not reported	None	1 patient in ICG group with intra-operative bleeding needing placement of additional trocar
Schols et al. (42)	2013	15	Comparative case series	Laparoscopic	2.5 mg	After intubation	Storz	100% (15/15)	100% (15/15)	None	No post-operative adverse events
Schols et al. (43)	2013	30	Case series	Laparoscopic	2.5 mg	After intubation/ during surgery	Storz	97% (29/30)	83% (25/30)	None	1 conversion from laparoscopic to open for
Spinoglio et al. (44)	2013	45	Case series	SIRS	2.5 mg	30 min before surgery	Intuitiv	98% (44/45)	CBD 91% (41/45), CHD 89% (40/45)	None	No post-operative adverse events
Verbeek et al. (45)	2014	14	Case series	Laparoscopic	5 or 10 mg	30 min or 24 hr before surgery	Storz	100% (14/14)	Not reported	Not reported	Not reported

Table 2 (*continued*)

Table 2 (*continued*)

Author	Year	n	Study design	Surgery	ICG dose	Timing	Fluorescence imaging system	IR of CD (%)	IR of CBD/CHD (%)	Complications of dye injection	Post-operative outcomes
Prevot et al. (46)	2014	23	Case series	Laparoscopic	0.05 mg/kg	After intubation	Storz	100% (23/23)	78% (18/23)	None	1 abscess
Daskalaki et al. (47)	2014	184	Case series	Robotic	2.5 mg	45 min before surgery	Intuitiv	98% (184/188)	CBD 96% (177/184), CHD 94% (173/184)	None	3.3% (6/184), 3 medical, 3 hepatic fluid collections
Larsen et al. (48)	2014	35	Case series	Laparoscopic	0.3–0.4 mg/mL/kg	After intubation	Olympus	100% (35/35)	100% (35/35)	None	No post-operative adverse events
Boni et al. (49)	2015	52	Case series	Laparoscopic	0.4 mg/mL/kg	15 min before surgery/during surgery	Storz	100% (52/52)	100% (52/52)	None	Not reported
Dip et al. (50)	2014	43	Comparative case series	Laparoscopic	0.05 mg/kg	60 min before surgery	Storz	98% (42/43)	CBD 79.1% (34/43), CHD 58.1% (25/43)	None	Not reported
Osayi et al. (51)	2015	82	Case series	Laparoscopic	2.5 mg	60 min before surgery	Stryker	95% (78/82)	CBD 77% (63/82), CHD 70% (57/82)	None	No post-operative adverse events
Dip et al. (52)	2015	45	Comparative case series	Laparoscopic	0.05 mg/kg	60 min before surgery	Storz	100% (45/45)	CBD 80% (36/45), CHD 60% (27/45)	None	No post-operative adverse events
VanDam et al. (53)	2015	30	Comparative Case series	Laparoscopic	0.05 mg/kg	After intubation	Olympus	97% (29/30)	86.7% (26/30)	None	1 post-operative biloma needing ERCP
Kono et al. (54)	2015	108	Comparative case series	Laparoscopic	2.5 mg	30 min before surgery/during surgery	Hammamatsu, Olympus, HD version of Hammamatsu, Storz, Novadaq pinpoint	95% (103/108)	93% (100/108)	None	Not reported
Dip et al. (55)	2016	71	Case series	Laparoscopic	0.05 mg/kg	60 min before surgery	Storz	100% (71/71)	CBD 71.8% (51/71), CHD 70.4% (50/71)	None	No post-operative adverse events

Table 2 (*continued*)

Table 2 (*continued*)

Author	Year	n	Study design	Surgery	ICG dose	Timing	Fluorescence imaging system	IR of CD (%)	IR of CBD/CHD (%)	Complications of dye injection	Post-operative outcomes
Zroback et al. (56)	2016	12	Case series	Laparoscopic	3.75 mg	In pre-operative holding area	Novadaq	100% (12/12)	CBD 83% (10/12), CHD 50% (6/12)	None	1 subtotal cholecystectomy, 1 post-operative bleeding from cystic artery needing embolization
Zarrinpar et al. (57)	2016	37	Comparative case series	Laparoscopic	0.02, 0.04, 0.08, 0.25 mg/kg	10 min, 15 min, 1 hour	Novadaq	Not reported	Not reported	None	No post-operative adverse events
Igami et al. (58)	2016	21	Case series	SILS	2.5 mg	After intubation	Storz	100% (21/21)	81% (17/21)	None	1 urethreal injury
Boogerd et al. (59)	2016	25	Case series	Laparoscopic	5 or 10 mg	30 minutes, 2, 4, or 6 hours before surgery	Storz	96% (24/25)	Not reported	None	No post-operative adverse events
Graves (60)	2017	11	Case series	Laparoscopic	0.025 mg	Direct GB injection on table	Stryker	91% (10/11)	91% (10/11)	None	Not reported
Maker et al. (61)	2017	35	Case series	Robotic	2.5 mg	After intubation	DaVinci	100% (35/35)	100% (35/35)	Not reported	Not reported
Liu et al. (62)	2018	46	Case series	Laparoscopic	1.25 mg	Direct GB injection on table	Storz	87.0% (40/46)	78.3% (36/46)	None	No post-operative adverse events
Hiwatashi et al. (63)	2018	65	Case series	Laparoscopic	2.5 mg	2 hr before surgery	Storz	83.1% (54/65)	93.8% (61/64)	None	No post-operative adverse events
Yoshiya et al. (64)	2019	39	Comparative case series	Laparoscopic	2.5 mg	After intubation	Storz	Not reported	Not reported	Not reported	10% complication (4/39)
Ambe et al. (65)	2019	29	Comparative case series	Laparoscopic	1.25 mg	60 min before surgery	Novadaq	Not reported	Not reported	None	No post-operative adverse events

SILS, single incision laparoscopic surgery; GB, gallbladder; IR, identification rate; CBD, common bile duct; CHD, common hepatic duct.

quality of the image that the surgeon can use. As these variables are heterogenous, it is difficult to directly compare them. Consensus of the available literature in this specific application of ICG FGS is very encouraging. Compared to bright-light surgery, most studies found that the use of ICG fluorescence guidance led to a higher identification rate of the cystic duct, the CD-CBD junction, the CVS, a shorter time to identification of vital structures, clearer dissection plane between the gallbladder and hepatic fossa, and improved identification of accessory hepatic ducts or recognition of aberrant anatomy if present. Boni *et al.* comment that they were able to identify the biliary anatomy in all cases where ICG was used, irrespective of whether the tissue was normal or inflamed (49). Contrary to this, Hiwatashi *et al.* noted that the group in which the CD was not identified, had a higher likelihood of inflammatory markers and clinical diagnosis of acute cholecystitis (63).

While the data on outcomes is even more limited, of the groups that report it, there were no major adverse reactions to dye administration and there were decreased rates of conversion to open surgery, decreased rates of subtotal cholecystectomies, shorter operative times. Schols *et al.* reported significantly earlier identification of the CD (ICG 23 min *vs.* standard 31 min, P=0.004) and the CBD (ICG 22 min *vs.* standard 32 min, P=0.001) (42). Buchs *et al.* found a significantly shorter operative time by 24 min compared to standard bright light single-incision robotic cholecystectomy (P=0.06) (41). While they did not report identification rates, they noted that the decreased operative time was attributable to earlier identification of the CVS. This difference was significant only for patients with body-mass index (BMI) less than 24 as the thickness of the fat pad around the biliary tree led to limited ICG penetration and optimal CVS visualization. This was also supported by work by Daskalaki and Osayi *et al.* that specifically looked at group stratification by BMI.

As fluorescence-based IOC has little risk, the cost of the dye itself is low, and fluorescence-enabled laparoscopes are more widely available, many surgeons familiar with fluorescence technology favor its routine use. Proponents of FGS technology argue that the barrier to use of fluorescence-based cholangiography is low and technical feasibility is uncomplicated. The cost-effectiveness of this approach was evaluated by Dip et al, comparing the cost of IOC and fluorescence-based IOC (52). They found that the use of fluorescence IOC was more cost effective when compared to IOC at 13.97±4.3 USD *vs.* 778.43±0.4 USD per patient (P=0.0001) without the need to cannulate the

CD. They note that the cannulation of the CD is one of the main points of contention by those who are adverse to routine IOC to prevent bile duct injury. If the wrong duct has been identified and cannulated, an IOC will prevent further injury such as complete transection of the CBD, but the choledochotomy will still need to be repaired.

However, incidences of biliary injuries during standard laparoscopic cholecystectomy are low and selective IOC is now preferred in most centers. There is not yet enough data to determine if fluorescence-cholangiography will affect rates of bile duct injury and or overall patient outcomes. Studies are ongoing to determine the added value of fluorescence cholangiography compared to conventional laparoscopic cholecystectomy. A number of studies compared fluorescent cholangiogram to IOC, while others compared FGS to standard bright light surgery (*Table 3*). Common end points are "time to identification of critical view of safety" "rate of identification of anatomic structures" and common secondary end points are "OR time", "outcomes", and "cost".

ICG for visualizing bile leaks

Besides IOC, ICG is useful in evaluating the biliary system during hepatic resections as a tool for evaluating bile leaks. While the use of ICG for visualizing intrahepatic bile ducts is limited due to tissue depth penetration, it is useful to evaluate details over the cut surface of the liver. Kaibori *et al.* and Sakaguchi *et al.* both described the approach using a cholangiocatheter cannulation of the cystic duct stump to deliver ICG (66,67). Both studies showed that the use of ICG led to increased rates of detection of bile leaks compared to standard of care using a saline or fat emulsion injection. After repair, this led to no post-operative bile leaks in the ICG group in both studies compared to 6% and 10% respectively in the standard of care groups. The use of fluorescence imaging over the surgical bed of hepatic resections increased the rate of detection of bile leaks and subsequent complications.

ICG for visualizing hepatic segments

Anatomic resection of the liver based on Couinad segments revolutionized liver surgery by allowing surgeons to be methodical about the tissue that is removed while preserving healthy parenchyma (68). While intraoperative ultrasound is useful in visualizing the adjacent relationships of the vasculature, biliary structures and the lesion to be removed

Table 3 Summary current clinical trials using ICG for cholecystectomy

Clinical trial ID	Title	Institution	Investigator	n	Design	Dose	Timing	Fluorescence imaging system	Comparator	End points
NCT02070627	Near infrared fluorescence cholangiography (NIRF-C) during cholecystectomy—use in acute cholecystitis sub-study	Ohio State	Vimal et al.	6	Open label single arm	2.5 mg	30–60 min before surgery	Stryker	ICG vs. IOC	Adverse events; anatomic ID rate; OR time
NCT02070640	Near infrared fluorescence cholangiography (NIRF-C) during cholecystectomy	Ohio State	Vimal et al.	99	Open label single arm	2.5 mg	30–60 min before surgery	Stryker	ICG vs. IOC	Adverse events; anatomic ID rate; OR time
NCT02344654	Fluorescence cholangiography during cholecystectomy-a RCT	Hvidovre niversity Hospital	Lehrskov et al.	120	Randomized parallel, open label	0.05 mg/kg	After intubation	Not identified	ICG vs. IOC	ID rate of CD; time spent on fluorescence cholangiogram vs. IOC; surgeon satisfaction; adverse events; cost
NCT01424215	The use of fluorescent imaging for intraoperative cholangiogram during laparoscopic cholecystectomy	Maimonides Medical Center	Sherwinter et al.	100	Randomized parallel, open label	Not identified	Not identified	Novadaq	ICG vs. standard laparoscopic cholecystectomy	OR time; adverse events; time to ID anatomic structures; autonomy to residents
NCT03812432	Cholecystocholangiography by direct intragallbladder injection of ICG	Hospital Son Espases	Romero et al.	80	Open label single arm	Not identified	On table	VISERA ELITE II	Not identified	ID rate of anatomic structures
NCT02558556	FALCON: a multicenter randomized controlled trial	Maastricht University Medical Center	Van den Bos et al.	308	Randomized parallel, open label	2.5 mg	After intubation	Storz	ICG vs. standard laparoscopic cholecystectomy	Time to ID CVS; time to ID CD-CBD junction; ID rate of anatomic structures; OR time
NCT01410734	Fluorescence imaging on the da Vinci surgical system for intra-operative near infrared imaging of the biliary tree	Multi-centered: Italy, Switzerland	Intuitiv Surgical	72	Open label single arm	2.5 mg	30 min before surgery	da Vinci	Not identified	ID rate of anatomic structures; outcomes
NCT02702843	Fluorescent cholangiography vs. white light for bile ducts identification	Multi-centered: US, Argentina, Germany, Italy, Japan	Rosenthal et al.	1,000	Randomized parallel, open label	Not identified	Not identified	Not identified	ICG vs. standard laparoscopic cholecystectomy	ID rate of anatomic structures; outcomes
NCT01881399	Fluorescence versus intraoperative cholangiography in the visualization of biliary tree anatomy (FLARIOC)	Service de Chirurgie Digestive et Endocrinienne-Nouvel Hôpital Civil	Pessaux et al.	66	Open label single arm	5 mg	Intraop	da Vinci	ICG vs. IOC	ID rate of CD-CBD junction vs. IOC; accuracy of identification due to fluorescence; accuracy of identification due to augmented overlay; time to identification

in real-time, the determination of resection boundaries at the level of hepatic surface anatomy is still often difficult to determine. A variety of techniques have been used to better delineate the anatomic segments prior to initiating parenchymal transection. Selective ligation of vascular pedicles and subsequent visualization of the ischemic boundaries is one approach. Dye injection as demonstrated by Makuuchi is another (69). A major issue with the use of traditional dyes such as MB and indigo-carmine, is the rapid washout after injection. The active transport of ICG and liver specificity of its metabolism allow the fluorescence signal from ICG to persist throughout the operation for continued image guidance. Aoki *et al.* and Inoue *et al.* first showed the feasibility of this approach, especially when following the intersegmental planes during division of the liver parenchyma (70,71). Twelve out of the 33 papers relevant to FGS hepatic resections looked at segmental staining to help guide parenchymal resection (*Table 4*). These are given as either standard doses of 2.5–5 mg or weight-based at 0.25–0.5 mg/kg. Administration of the dye can be performed intraoperatively. Positive segmental staining can be obtained by selective portal vein injection while negative segmental staining can be obtained by intravenous injection during selective portal clamping. While there is increasing literature describing surgeons' experiences and case series in this area, there is little to no information on outcomes. As technology and experience with this approach expands the information should be forthcoming.

ICG for visualizing hepatic tumors

The vasculature of neoplastic tissue is leaky and poorly organized, an effect called the EPR effect (103). This leads to retention of ICG in distinct patterns with certain HPB neoplasms that lend itself to utility in fluorescence-guided oncologic procedures. Ishizawa and Gotoh were the first groups to describe the use of ICG fluorescence to localize hepatic lesions (72,73). Patients received intravenous ICG as part of a routine pre-operative liver function assessment and the persistent signal at the tumors from this test was used to navigate resection margins. Twenty-one out of the 33 articles relevant to ICG fluorescence hepatectomy used this approach to label the tumor for intra-operative guidance. Gotoh *et al.* described HCC lesions as a bright homogenous fluorescence signal (72). They were able to detect all 10/10 pre-operatively diagnosed lesions, and in eight cases, new surface nodules not detected by either pre-operative imaging or IOUS were detected with the use of fluorescence

imaging, 4/8 were HCC. Ishizawa described 37 patients with HCC and 12 patients with CLM, 23 of whom had the specimen imaged after resection with fluorescence imaging and 26 had real-time intra-operative fluorescence imaging after hepatic mobilization. They described three patterns of fluorescence: a bright homogenous fluorescence signal seen most commonly with HCC lesions, partial fluorescence seen in HCC lesions with components of hemorrhagic necrosis, and ring type fluorescence seen in CLM. Fluorescence microscopy for HCC lesions showed that the fluorescence was within the cancerous cells whereas in CLM lesions, the fluorescence was located at the surrounding non-cancerous liver parenchyma compressed by the tumor. *Figure 1* adapted from Ishizawa's review on ICG fluorescence imaging for HPB cancer shows these fluorescence patterns (104). Uchiyama used ICG in conjunction with contrast-enhanced IOUS to detect CLM and found that these lesions did not fluoresce homogenously compared to HCC and most were ring enhancing (n=18) (74). They found that the sensitivity of contrast-enhanced IOUS in conjunction with ICG fluorescence imaging was superior to multiple detector computed tomography (MDCT)/magnetic resonance imaging (MRI), 98.1% *vs*. 88.5% (P=0.05). They saw that even lesions that radiographically disappeared with neoadjuvant chemotherapy still showed a fluorescence signal and were positive for microscopically-viable cancer cells on pathology. Boogerd *et al.* reported on the use of ICG for hepatic resection of a wide variety of lesions including intrahepatic cholangiocarcinoma and hepatic metastases of uveal melanoma and breast cancer (59). These lesions showed a rim type fluorescence similar to CLM lesions.

Since the initial report of the use of ICG in hepatic resections, several hundred cases have been reported with a variety of timing and dosing of administration and overall, a good sensitivity ranging from 70–100% up to 10 mm depth (105). While the safety and efficacy of ICG administration has been well reported, the long-term outcomes after fluorescence-guided hepatic resection compared to conventional resection is unclear. Handgraaf *et al.* showed that the use of fluorescence imaging increased the number of additional lesions detected during surgery for CLM to 25% from 13% (P=0.04) and the lesions detected by fluorescence imaging were usually smaller 3.2±1.8 *vs*. 7.4±2.6 mm (P<0.001) (106). While was an improvement in liver-specific recurrence-free survival at 4 years of 47% using fluorescence compared to 39% with conventional surgery, the study was not powered sufficiently to detect a significant difference. Further studies will need

Table 4 Summary of studies using ICG for hepatectomy

Authors	Year	n	Dose	Route	Timing	Fluorescence imaging system	Surgery	Tumors	Staining type
Aoki et al. (70)	2008	35	5 mg	Injection into PV branch	Intraop	Hammamatsu	Open	13 HCC, 18 liver metastases, 4 CholangioCA	Segmental stain
Gotoh et al. (72)	2009	10	0.5 mg/kg	Intravenous	1–8 days before surgery	Hammamatsu	Open	10 HCC	Tumor stain
Ishizawa et al. (73)	2009	26	0.5 mg/kg	Intravenous	1–7 days before surgery	Hammamatsu	Open	20 HCC, 6 CLM	Tumor stain
Aoki et al. (36)	2010	81	5 mg	Injection into PV branch	Intraop	Hammamatsu	Open	28 HCC, 35 CLM, 8 CholangioCA, 10 other	Segmental stain
Uchiyama et al. (74)	2010	32	0.5 mg/kg	Intravenous	2 weeks before surgery	Hammamatsu	Open	32 CLM	Tumor stain
Uchiyama et al. (75)	2011	22	0.5 mg/kg	Intravenous	After ligation of portal pedicle	Hammamatsu	Open	22 HCC	Segmental stain
Ishizuka et al. (76)	2012	7	0.1 mg/kg/mL	Intravenous	Not reported	Hammamatsu	Open	7 CLM	Tumor stain
Peloso et al. (77)	2013	25	0.5 mg/kg	Intravenous	24 hours before surgery	Hammamatsu	Open	25 CLM	Tumor stain
Tanaka et al. (78)	2013	33	0.5 mg/kg	Intravenous	2 days before surgery	Hammamatsu	Open	10 cirrhotic livers, 23 non-cirrhotic (specifically 12 HCC, 9 CLM, 1 CholangioCA, 1 hepatic carcinoid)	Tumor stain
Kudo et al. (79)	2014	17	0.5 mg/kg	Intravenous	2 weeks before surgery	Olympus	Laparoscopic	10 HCC, 6 CLM, 1 uterine cancer	Tumor stain
Sakoda et al. (80)	2014	2	5 mg	Injection into PV branch	Intraop	Olympus	Laparoscopic	2 HCC	Segmental stain
Tummers et al. (81)	2015	3	10 mg	Intravenous	1 day before surgery	Storz	Laparoscopic	3 uveal melanoma	Tumor stain
Yamamichi et al. (82)	2015	3	0.5 mg/kg	Intravenous	2–3 days before surgery	HyperEye	Open	3 hepatoblastoma	Tumor stain
Barabino et al. (83)	2016	3	0.25 mg/kg	Intravenous	24 hours before surgery	Fluoptics	Open	2 endocrine liver metastasis, 1 CLM	Tumor stain
Kaibori et al. (84)	2016	48	0.5 mg/kg	Intravenous	14 days before surgery	Hammamatsu	Open	31 HCC, 13 CLM, 2 CholangioCA, 2 benign	Tumor stain
Takahashi et al. (85)	2016	15	5–7.5 mg	Intravenous	1–2 days before surgery	Intuitive, Novadaq	Open, laparoscopic, robotic	9 CLM, 2 neuroendocrine, 1 FNH, 1 hemangioma	Tumor stain
Zhang et al. (86)	2017	50	0.25 mg/kg	Injection into PV, Rt gastric vein, central venous catheter	Intraop	Hammamatsu	Open	38 HCC, 4 cavernous hemangiona, 3 CholangioCA, 2 CLM, 1 Malignant fibrous histiocytoma, 2 micronodular cirrhosis	Segmental stain
Kawaguchi et al. (87)	2017	21	2.5 µg/mL of total liver volume estimated from 3D CT	Intravenous after segmental HV, PV, HA clamping	Intraop	Hammamatsu	Open	9 HCC, 9 CLM, 3 others	Segmental stain

Table 4 (*continued*)

Table 4 (*continued*)

Authors	Year	n	Dose	Route	Timing	Fluorescence imaging system	Surgery	Tumors	Staining type
Terasawa *et al.* (88)	2017	41	0.5 mg/kg preoperatively, 1.25 mg intraoperatively	Intravenous	3 days before surgery and intraop	Novadaq	Laparoscopic	7 HCC, 46 CLM, 6 others	Tumor stain
Narasaki *et al.* (89)	2017	16	2.5 mg/L of estimated liver volume	Intravenous	intraop	Mini-FLARE	Open	6 CholangioCA, 5 GB cancer, 2 pancreatic cancer, 1 ampullary cancer, 1 CLM, 1 renal cancer	Segmental stain
Kobayashi *et al.* (90)	2017	105	0.25 mg ICG diluted with indigocarmine or 2.5 mg ICG	Intravenous or injection into PV branch	Intraop	Hammamatsu	Open	71 HCC, 25 CLM, 5 CholangioCA, 2 other	Segmental stain
Lieto *et al.* (91)	2018	9	0.5 mg/kg	Intravenous	1 day before surgery	Fluoptics	Open	3 HCC, 6 CLM	Tumor stain
Nanashima *et al.* (92)	2018	3	0.5 mg/kg	Intravenous	"Several days" before surgery	Hammamatsu	Open	3 HCC	Tumor stain
Cheung *et al.* (93)	2018	20	0.5 mg/kg	Intravenous	10–14 days before surgery	Novadaq	Laparoscopic	20 HCC	Tumor stain
Peyrat *et al.* (94)	2018	43	0.25 mg/kg, additional dilute injections intraoperatively	Intravenous, PV injection intraop	1 day before surgery, Intraop	Fluoptics	Open	2 HCC, 2 CholangioCA, 36 CLM, 3 other	Tumor stain
Nomi *et al.* (95)	2018	16	1.5 mg	Intravenous	Intraop	Novadaq	Laparoscopic	Not reported	Segmental stain
Chiba *et al.* (96)	2018	24	Not reported	Injection into cystic artery	Intraop	HyperEye	Open	24 GB cancer	Segmental stain
Alfano *et al.* (97)	2019	27	0.5 mg/kg followed by 0.2 mg/kg if >7 days after 1st injection	Intravenous	1–7 days before surgery	Stryker	Open	19 HCC, 2 CholangioCA, 6 CLM	Tumor stain
He *et al.* (98)	2019	2	0.5 mg/kg	Intravenous	72–96 hr before surgery	Hammamatsu	Open	2 HCC	Tumor stain
Urade *et al.* (99)	2019	3	2.5 mg	Intravenous	Intraop	Olympus	Laparoscopic	2 HCC, 1 liver metastasis	Segmental stain
Souzaki *et al.* (100)	2019	5	0.5 mg/kg	Intravenous	18–138 hours before surgery	Not reported	Open, VATS	5 hepatoblastoma	Tumor stain
Yoshioka *et al.* (101)	2019	1	0.5 mg/kg	Intravenous	2 days before surgery	Novadaq	Laparoscopic	1 HCC recurrent	Tumor stain
Marino *et al.* (102)	2019	20	2.5 mg	Injection into PV branch	Intraop	Intuitive	Robotic	Not reported	Segmental stain

PV, portal vein; VATS, video assisted thoracoscopic surgery; HCC, hepatocellular carcinoma; CLM, colorectal liver metastasis; CholangioCA, cholangiocarcinoma.
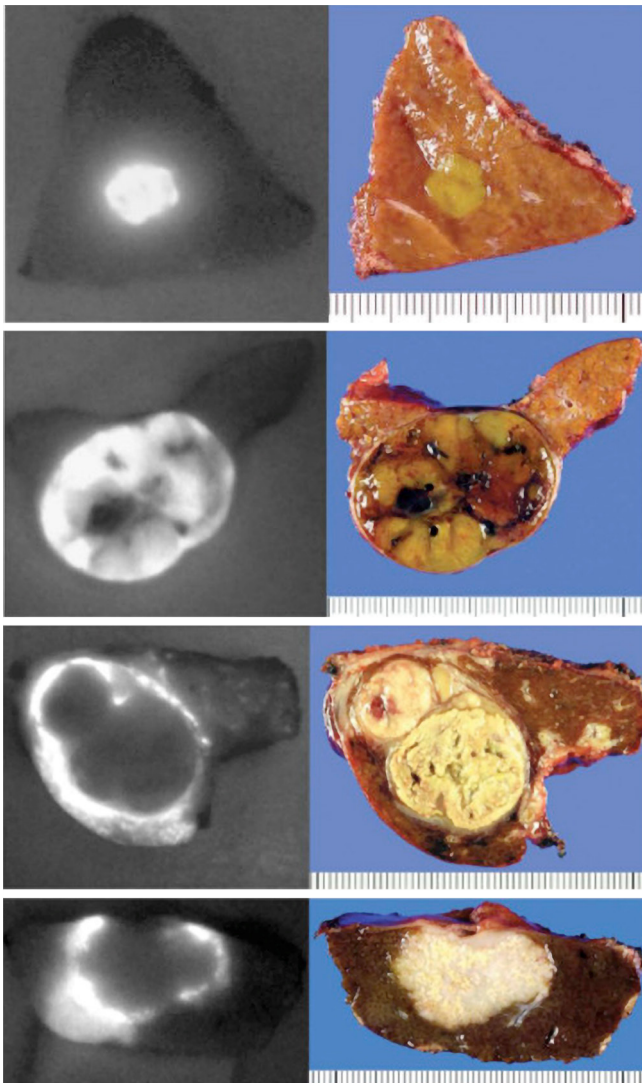
Figure 1 Differential patterns of fluorescence signals on the cut surface of different liver cancers using ICG. ICG administered pre-operatively gives a fluorescence signal over the liver when imaged with a NIR-fluorescence camera. The patterns can be classified into bright homogenous "total" fluorescence type (A) well-differentiated hepatocellular carcinoma (HCC), partial fluorescence type (B) moderately differentiated HCC, and rim-type fluorescence (C), poorly differentiated HCC (upper) and CLM (lower). Adapted from (104). ICG, indocyanine green; CLM, colorectal liver metastases.

to be performed to determine the long-term outcomes of fluorescence guided oncologic surgery.

ICG and minimally invasive liver surgery

Fluorescence navigation using a NIR wavelength is well-suited for minimally-invasive liver surgery since this is already an environment where the surgeon is interacting with a monitor for visualization. Within four years of introduction of NIR fluorescence technology to open surgeries, NIR-enabled fluorescence laparoscopes were commercially available. In 2012, Ishizawa *et al.* first reported the initial experience of laparoscopic fluorescence-imaging guidance to delineate hepatic segments during resection (107). Kudo *et al.* reported in 2014 on the first series of patients undergoing laparoscopic hepatectomy using a positive fluorescence signal to identify the liver surface tumors (79). Of the 33 papers identified using ICG for FGS of liver lesions, 10 discuss using a minimally-invasive approach, either laparoscopic or robotic. Authors of these studies especially note that the use of fluorescence in laparoscopy was especially useful for identifying small sub-centimeter sub-capsular lesions that were not readily evident under bright-light visualization (108). They note the added benefit of fluorescence for visualization in these minimally-invasive approaches, especially that contrast enhancement compensates for the inability of the surgeon receive manual tactile feedback. Additionally image guidance was useful at superficial depths where IOUS may not readily detect these lesions. Fluorescence-navigation technology assisted in increasing the sensitivity of detecting lesions and localizing the resection margins in minimally-invasive settings.

Currently ongoing clinical trials using ICG in liver surgery are summarized in *Table 5*, however the work is still limited, focusing on feasibility, accuracy, and detections rates. There is limited information on outcomes, but with further experience, as well as expansion and maturation of this technology, more data should become available.

ICG in liver transplants

The ability to use ICG to delineate boundaries of liver segments, visualize the biliary tree and directly assess perfusion without directly cannulating the vasculature makes it uniquely applicable to the field of transplant surgery in both living donor liver transplants (LDLT) and for liver transplant recipients in general. The technology allows donor liver parenchyma to be precisely transected at the segmental interfaces, identify aberrant anatomy, check for bile leaks and evaluate the perfusion and function of the residual liver after donor partial hepatectomy. Mizuno *et al.* first used ICG to delineate aberrant anatomy in a

Table 5 Summary current clinical trials using ICG for hepatectomy

Clinical trial ID	Title	Investigator	Institution	n	Design	Dose	Timing	Fluorescence imaging system	Comparator	End points
NCT01738217	Assessment of indocyanine green as a near-infrared fluorescent contrast agent for image-guided liver surgery (HEPATOFLUO)	Peyrat et al.	Centre Leon Berard	48	Open label single arm	Not identified	Not identified	Fluobeam	Not applicable	Evaluate feasibility and acceptability of device
NCT03811704	Real-time navigation for laparoscope liver resections using fusion 3d imaging and indocyanine green fluorescence imaging	Fang et al.	Zhujiang Hospital	50	Open label single arm	Not identified	Not identified	Novel augmented reality surgery navigation system (ARSNS)	Not applicable	Feasibility of ARSNS for surgical navigation
NCT03579199	Practical application of indocyanine green camera in laparoscopic liver surgery (CAMVIC)	Vibert et al.	Centre Hépato Biliaire de l'hopital Paul Brousse	120	Open label single arm	Not identified	Not identified	Not identified	Not applicable	Number of superficial nodules detected compared to pre-op imaging; number of new surface nodules at 6 months
NCT03793322	The application of indocyanine-green (ICG) fluorescence imaging in hepatocellular carcinoma	Fang et al.	Zhujiang Hospital	100	Open label single arm	Not identified	1 day before surgery or intraop	Not identified	Not applicable	Accuracy of detection of small liver tumors; detection of positive margins as confirmed by histology

LDLT and further expand the application by using ICG fluorescent-cholangiogram to determine the point of transection of the bile duct (109,110). For liver transplant recipients, the technology allows surgeons to directly evaluate vascular anastomoses without instrumentation or cannulation, check for bile leaks and additionally gives an indicator of synthetic function as the fluorophore undergoes biliary excretion. Kubota *et al.* first used this technology in 3 patients receiving LDLT to evaluate vascular anastomoses (111). Recipients were imaged 10 seconds after injection and showed adequate flow through both the hepatic artery and portal vein. Forty minutes after the initial injection, there was biliary excretion of the dye showing appropriate biliary function and all patients recovered uneventfully. Figueroa *et al.* reported on the largest study of liver recipients using this technology: 72 patients received intravenous injections of ICG and perfusion patterns over the liver surface were evaluated and categorized as homogenous, non-perfused areas, and patchy perfusion throughout (112). Patients with patchy perfusion had a higher rate of primary graft dysfunction of 60% compared to patients with non-perfused areas (30%) and patients with homogenous perfusion (17%).

Tumor-specific fluorescence imaging for HPB surgery

While imaging with fluorophores alone is useful for evaluating surface anatomy of the liver and visualizing hepatic lesions, the technology is sensitive, but not specific. Not all nodules that exhibit a fluorescence signal are malignant. While we are still accumulating more knowledge on the use of fluorescence pattern recognition, especially using ICG, there is not one signal intensity or pattern that clearly indicates malignancy. While the decision is clear for fluorescent lesions that clearly correlate with pre-operative imaging, it is unclear what to do for these indeterminate lesions where the location may change the extent of planned surgery. The technology often identifies additional lesions and after these lesions are resected, histologic examination shows that not all are malignant. Case-series reporting on additional lesions discovered by NIR fluorescence imaging describe false-positive fluorescent nodules, especially in the setting of cirrhosis. False positive rates are variable and can be as high as 40% and up to 87% in cirrhotic livers (78). Tanaka *et al.* report that the positive predictive value of ICG in cirrhotic livers can be as low as 5.4% compared to 100% in healthy livers (78). While those numbers are extreme, most groups use a combination of clinical judgment, bright-
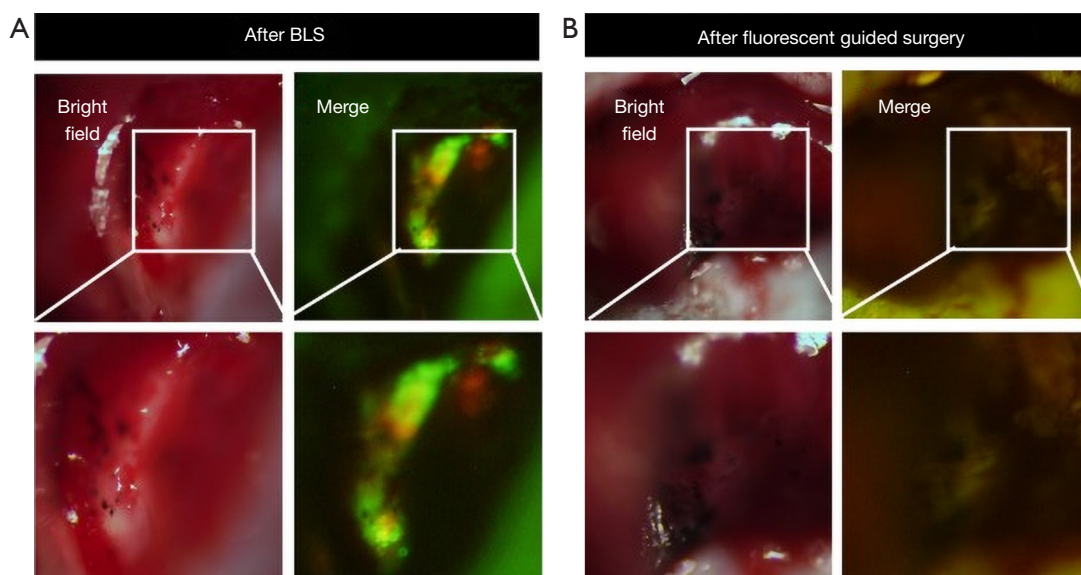
Figure 2 Visualizing a liver metastasis with viral-GFP in an orthotopic model of colon cancer. OBP-401, a conditionally-replicative adenovirus expressing GFP, was injected into orthotopically-implanted colorectal liver metastases 3 days before surgical resection. After BLS, both a GFP fluorescence signal from OBP-401 and an RFP signal from RFP-labeled cells were detected in the surgical bed (A). After OBP-401-FGS, there were no residual cancer cells (B). Adapted from (117). GFP, green fluorescence protein.

light inspection, and contrast enhanced IOUS to indicate malignancy prior to resection (88).

The use of tumor-binding probes conjugated to fluorophores can confer further specificity to FGS. These probes use a variety of mechanisms to confer specificity to lesions. The most common approach is targeting using antigen-antibody binding, but other approaches such as peptide binding, selective protease activation, pH differential, or aberrant tumor metabolism are all viable techniques to selectively deliver a fluorescence signal to the target lesions while decreasing background noise.

Our lab has developed orthotopic mouse models of hepatic cancers, especially CLM (113-115). By either orthotopically implanting the tumor specimen or additionally serially selecting for cell line variants that form hepatic metastases, we are able to create clinically-relevant mouse models for use in further establish of tumor-specific fluorescence platforms (116).

Yano *et al.* used a genetically-engineered adenovirus expressing green fluorescence protein (GFP) with an orthotopic CLM mouse model to show efficacy for FGS (117). The adenovirus called OBP-401, is a conditionally-replicative adenovirus with the replication cassette under the control of the human telomerase reverse transcriptase (hTERT) promoter and a GFP gene under the

control of a cytomegalovirus (CMV) promoter (118). The virus was administered directly into the tumor and imaging was performed 3 days after injection. A strong GFP signal was visualized at the tumor for FGS. The localization of OBP-401 GFP correlated with the red fluorescence protein (RFP) cells. Two groups of mice (n=16) underwent FGS *vs.* standard bright light surgery (BLS) and were evaluated 120 days after surgery. After BLS, there was still residual tumor at the surgical bed as indicated by GFP and RFP signals using fluorescence imaging (*Figure 2A*), but after FGS using OBP-401, there was no residual cancer remaining (*Figure 2B*). 94% (15/16) mice that underwent BLS had large tumor recurrences compared to mice that underwent FGS 19% (3/16) (P<0.001).

Hiroshima *et al.* also compared FGS *vs.* BLS using a orthotopic CLM model, but delivered fluorescence to the tumor with an intravenous injection of anti-carcinoembryonic antigen (CEA) antibody conjugated to a 650 nm fluorophore (119). The antibody-fluorophore conjugate was successful at delineating the tumor over the liver with a best signal to noise ratio at 72 hours. After BLS, there was still residual tumor at the surgical bed compared to FGS under anti-CEA-DyLight650 navigation where no residual cancer was detectable (*Figure 3A*). Additionally, the wavelength of the dye showed
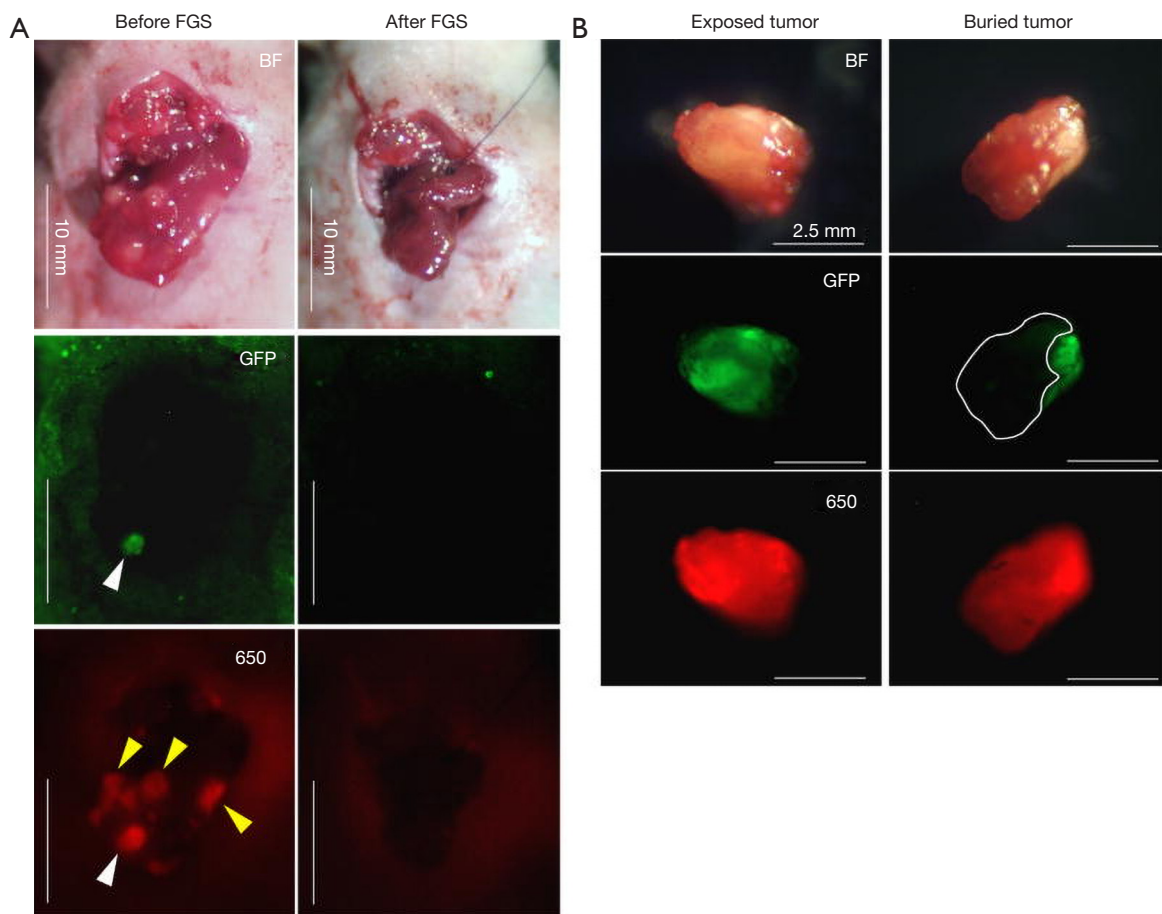
Figure 3 Visualizing a liver metastasis in an orthotopic model of colon cancer with a fluorescent antibody. Comparison between visible wavelength fluorescence and near-infrared fluorescence signal using anti-CEA antibody conjugated to DyLight650 visualized using a Mini Maglite® LED Pro flash light (Mag Instrument) with an excitation filter (ET640/30X, Chroma Technology Corporation) and a Canon EOS 60D digital camera with an EF-S18-55 IS lens (Canon) and an emission filter (HQ700/75M-HCAR, Chroma Technology Corporation). (A) The surface-exposed tumor (white arrow head) was clearly detected under both GFP and anti-CEA-DyLight650 navigation. In contrast, the tumors covered with normal tissues (yellow arrow heads) were detected only under anti-CEA-DyLight650 navigation. No residual tumor was detected after FGS. (B) Representative gross images of excised tumors (left panel: exposed tumor, right panel: buried tumor). Upper panels indicate bright field (BF) images; middle and lower panels indicate fluorescence images for GFP and DyLight 650 [650], respectively. The area surrounded by a white broken line indicates the buried part of the excised tumor. CEA650 fluorescence was able to penetrate normal liver tissue and visualize the buried part of the tumor, which was not detected by GFP fluorescence. Scale bars: 10 mm (A) and 2.5 mm (B). Adapted from (119). CEA, carcinoembryonic antigen; GFP, green fluorescence protein.

an improved fluorescence signal penetration in the presence of overlying tissue compared to GFP (*Figure 3B*). Disease-free and overall survival were significantly higher in the FGS group compared to BLS. In these orthotopic mouse models of CLM, using tumor-specific fluorescence navigation for surgical resection, decreased the volume of residual disease and increased overall and disease-free survival.

Clinical translation of these approaches is rapid and underway (*Table 6*). Van Dam's group is evaluating the use of an anti-VEGF antibody conjugated to an 800 nm fluorophore, bevacizumab-800CW, in FGS of cholangiocarcinomas (NCT03620292). While the majority of these active clinical trials for tumor-specific probes are for colorectal and pancreatic cancers, the experience and concepts from these can be broadened into hepatic and biliary surgeries. Gutowski *et al.* report on

Table 6 Summary current clinical trials using tumor-specific probes

Tumor type	Probe	Clinical trial ID	Title	Institution	Investigator	n	Design	Dose	Timing	Fluorescence imaging system	Comparator	End points
CholangioCA	Bevacizumab-800CW	NCT03620292	Fluorescence image guided surgery in CholangioCA (COUGAR)	University Medical Center Groningen	Van Dam et al.	12	Open label dose finding	10, 25 or 50 mg of bevacizumab-800CW	3 days before surgery	Not identified	Dose	Optimal dose of Bevacizumab-800CW; comparison of per-operative vs. ex-vivo analysis; detection of hilar cholangiocarcinoma intraoperatively; probe distribution; fluorescence signal in surrounding tissue
Pancreatic cancer	Panitumumab-IRDye800	NCT03384238	Panitumumab-IRDye800 in patients with pancreatic cancer undergoing surgery	Stanford University	Rosenthal et al.	24	Open label single arm	Not identified	2–5 days before surgery	Novadaq devices: SPY/LUNA, Pinpoint, IR9000 fluorescence imaging system, and/or SurgVision Explorer Air	Not applicable	Tumor-to-background ratio; adverse events; number of positive lymph nodes not detected by white light; number of positive resection margins not detected by white light
Pancreatic cancer and metastatic colorectal cancer	SGM-101	NCT02973672	Phase I of SGM-101 in patients with cancer of the colon, rectum or pancreas	Center for human drug research, Netherlands, Leiden University Medical Center, Erasmus Medical Center	Burffraaf et al.	60	Open label single arm	Not identified	4 days before surgery	Not identified	Not applicable	Rate of adverse events; tumor-to-background ratio; serum SGM-101 concentration
Pancreatic cancer	Bevacizumab-800CW	NCT02743975	Near-infrared image guided surgery in pancreatic adenocarcinoma (PENGUIN)	University Medical Center Groningen	Van Dam et al.	26	Open label dose finding	4.5, 10, 25, or not 50 mg of bevacizumab-800CW	Not identified	Not identified	Dose	Mean fluorescence intensity in tumor vs. normal tissue; optimal dose; adverse events
Pancreatic cancer	Cetuximab-800CW	NCT02736578	Cetuximab-IRDye 800CW and intraoperative imaging in finding pancreatic cancer in patients undergoing surgery	Stanford University	Rosenthal et al.	8	Open label parallel of unlabeled cetuximab, 50 vs. 100 mg of labeled cetuximab	50 vs. 100 mg loading dose	2–5 days before surgery	Not identified	Dose	Assess dye uptake in tumor vs. non-cancerous tissue; measure fluorescence intensity; effect of dose on fluorescence intensity; sensitivity and specificity; detection in LNs; signal to noise ratios (ex vivo); signal to noise ratio (in vivo); toxicity

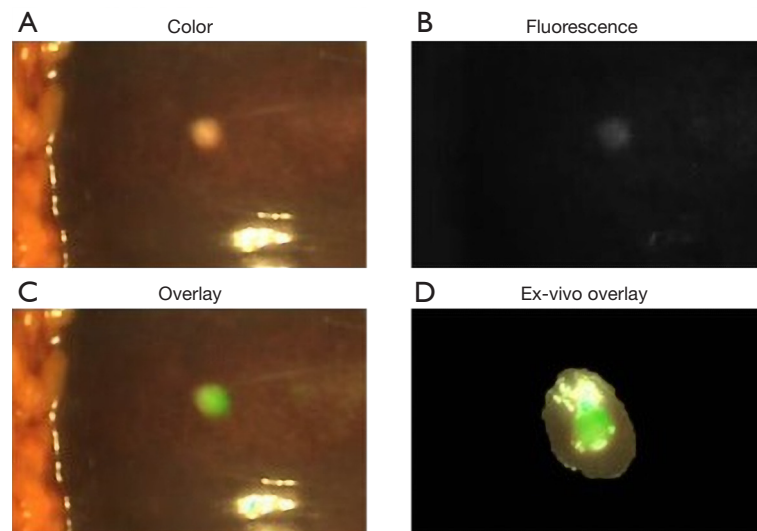CholangioCA, cholangiocarcinoma.

Figure 4 Fluorescence intraoperative imaging showing a liver metastasis of a pancreatic cancer using an anti-CEA antibody conjugated to SGM-101 near-infrared fluorophore using the Quest imaging system. Images shown in color (A), fluorescence (B), merged (C), and ex vivo imaging showing a slice from the same metastasis (D). Adapted from (122). CEA, carcinoembryonic antigen.

the results of clinical trial NCT02973672 using an anti-CEA antibody conjugated to a 700 nm dye called SGM-101 that successfully imaged colorectal and pancreatic cancers and this probe is advancing to a phase III clinical trial (120,121). SGM-101 was found also to be able to label CLM as well as pancreatic cancer metastases to the liver as shown in *Figure 4* (123). Rosenthal's group is working on an epidermal growth factor receptor (EGFR) conjugated to an 800 nm fluorophore for HPB and pancreatic cancers (NCT02736578, NCT03384238) (124-126).

These tumor-specific probes are still relatively early in their development, but the preliminary results are promising. With tumor-specific probes, there is enhanced and specific fluorescence at target lesions compared to a nonspecific dye such as ICG. Further work will need to be performed to optimize probe design, dose, schedule, and imaging devices. HPB procedures, especially those with minimally-invasive approaches, are cases where FGS can be used to potentially impact oncologic outcomes.

FGS is valuable for HPB surgery with both visible wavelength and NIR fluorophores. Nonspecific fluorophores are readily available and used in a variety of modalities to aid in visualization of desired structures. Non-specific accumulation at tumors helps localize the lesions at the surface as well as deeper within the parenchyma. Tumor-specific probes are a promising advancement in FGS with a greater degree of specificity. While advancing

rapidly, the technology is still relatively new and it will be very interesting to see its impact on outcomes in the next few years.

Acknowledgments

Footnote

Provenance and Peer Review: This article was commissioned by the Guest Editor (Dr. Yuman Fong) for the series "Imaging and HPB Surgery" published in *Hepatobiliary Surgery and Nutrition*. The article was sent for external peer review organized by the Guest Editor and the editorial office.

Reporting Checklist: The authors have completed the Narrative Review reporting checklist. Available at http://dx.doi.org/10.21037/hbsn.2019.09.13

Conflicts of Interest: All authors have completed the ICMJE uniform disclosure form (available at http://dx.doi.

org/10.21037/hbsn.2019.09.13). The series "Imaging and HPB Surgery" was commissioned by the editorial office without any funding or sponsorship. The authors have no other conflicts of interest to declare.

Ethical Statement: The authors are accountable for all aspects of the work in ensuring that questions related to the accuracy or integrity of any part of the work are appropriately investigated and resolved.

Open Access Statement: This is an Open Access article distributed in accordance with the Creative Commons Attribution-NonCommercial-NoDerivs 4.0 International License (CC BY-NC-ND 4.0), which permits the non-commercial replication and distribution of the article with the strict proviso that no changes or edits are made and the original work is properly cited (including links to both the formal publication through the relevant DOI and the license). See: https://creativecommons.org/licenses/by-nc-nd/4.0/.

References

1. Makuuchi M, Hasegawa H, Yamazaki S. Intraoperative ultrasonic examination for hepatectomy. Ultrasound Med Biol 1983;Suppl 2:493-7.

2. Clarke MP, Kane RA, Steele G, et al. Prospective comparison of preoperative imaging and intraoperative ultrasonography in the detection of liver tumors. Surgery 1989;106:849-55.

3. Hong G, Antaris AL, Dai H. Near-infrared fluorophores for biomedical imaging. Nat Biomed Eng 2017;1:s41551-016-0010-6.

4. Adams KE, Ke S, Kwon S, et al. Comparison of visible and near-infrared wavelength-excitable fluorescent dyes for molecular imaging of cancer. J Biomed Opt 2007;12:024017.

5. Zhu B, Sevick-Muraca EM. A review of performance of near-infrared fluorescence imaging devices used in clinical studies. Br J Radiol 2015;88:20140547.

6. Peek MC, Charalampoudis P, Anninga B, et al. Blue dye for identification of sentinel nodes in breast cancer and malignant melanoma: a systematic review and meta-analysis. Future Oncol 2017;13:455-67.

7. DiSanto AR, Wagner JG. Pharmacokinetics of highly ionized drugs. I. Methylene blue--whole blood, urine, and tissue assays. J Pharm Sci 1972;61:598-602.

8. Sari YS, Tunali V, Tomaoglu K, et al. Can bile duct injuries be prevented? "A new technique in laparoscopic

cholecystectomy". BMC Surg 2005;5:14.

9. Makuuchi M, Hasegawa H, Yamazaki S. Ultrasonically guided subsegmentectomy. Surg Gynecol Obstet 1985;161:346-50.

10. Shou-wang C, Shi-zhong Y, Wen-ping L, et al. Sustained methylene blue staining to guide anatomic hepatectomy for hepatocellular carcinoma: Initial experience and technical details. Surgery 2015;158:121-7.

11. Lam CM, Lo CM, Liu CL, et al. Biliary complications during liver resection. World J Surg 2001;25:1273-6.

12. Guillaud A, Pery C, Campillo B, et al. Incidence and predictive factors of clinically relevant bile leakage in the modern era of liver resections. HPB 2013;15:224-9.

13. Liu CL, Fan ST, Lo CM, et al. Safety of donor right hepatectomy without abdominal drainage: a prospective evaluation in 100 consecutive liver donors. Liver Transpl 2005;11:314-9.

14. Matsui A, Tanaka E, Choi HS, et al. Real-time intra-operative near-infrared fluorescence identification of the extrahepatic bile ducts using clinically available contrast agents. Surgery 2010;148:87-95.

15. Ashitate Y, Stockdale A, Choi HS, et al. Real-time simultaneous near-infrared fluorescence imaging of bile duct and arterial anatomy. J Surg Res 2012;176:7-13.

16. Stummer W, Suero Molina E. Fluorescence Imaging/Agents in Tumor Resection. Neurosurg Clin N Am 2017;28:569-83.

17. Hinnen P, de Rooij FW, van Velthuysen ML, et al. Biochemical basis of 5-aminolaevulinic acid-induced protoporphyrin IX accumulation: a study in patients with (pre)malignant lesions of the oesophagus. Br J Cancer 1998;78:679-82.

18. Stummer W, Pichlmeier U, Meinel T, et al. Fluorescence-guided surgery with 5-aminolevulinic acid for resection of malignant glioma: a randomised controlled multicentre phase III trial. Lancet Oncol 2006;7:392-401.

19. Fritsch C, Lang K, Neuse W, et al. Photodynamic diagnosis and therapy in dermatology. Skin Pharmacol Appl Skin Physiol 1998;11:358-73.

20. Denzinger S, Burger M, Walter B, et al. Clinically relevant reduction in risk of recurrence of superficial bladder cancer using 5-aminolevulinic acid-induced fluorescence diagnosis: 8-year results of prospective randomized study. Urology 2007;69:675-9.

21. Schneider ARJ, Zöpf T, Arnold JC, et al. Feasibility and diagnostic impact of fluorescence-based diagnostic laparoscopy in hepatocellular carcinoma: a case report. Endoscopy 2002;34:831-4.

22. Zöpf T, Schneider ARJ, Weickert U, et al. Improved preoperative tumor staging by 5-aminolevulinic acid induced fluorescence laparoscopy. Gastrointest Endosc 2005;62:763-7.

23. Inoue Y, Tanaka R, Komeda K, et al. Fluorescence detection of malignant liver tumors using 5-aminolevulinic acid-mediated photodynamic diagnosis: principles, technique, and clinical experience. World J Surg 2014;38:1786-94.

24. Inoue Y, Imai Y, Fujii K, et al. The utility of 5-aminolevulinic acid-mediated photodynamic diagnosis in the detection of intraoperative bile leakage. Am J Surg 2017;213:1077-82.

25. Honorato-Cia C, Martinez-Simón A, Cacho-Asenjo E, et al. Safety Profile of 5-Aminolevulinic Acid as a Surgical Adjunct in Clinical Practice: A Review of 207 Cases From 2008 to 2013. J Neurosurg Anesthesiol 2015;27:304-9.

26. Chung IWH, Eljamel S. Risk factors for developing oral 5-aminolevulinic acid-induced side effects in patients undergoing fluorescence guided resection. Photodiagnosis Photodyn Ther 2013;10:362-7.

27. Kamisaka K, Listowsky I, Betheil JJ, et al. Competitive binding of bilirubin, sulfobromophthalein, indocyanine green and other organic anions to human and bovine serum albumin. Biochim Biophys Acta 1974;365:169-80.

28. Hashimoto M, Watanabe G. Hepatic Parenchymal Cell Volume and the Indocyanine Green Tolerance Test. J Surg Res 2000;92:222-7.

29. Landsman ML, Kwant G, Mook GA, et al. Light-absorbing properties, stability, and spectral stabilization of indocyanine green. J Appl Physiol 1976;40:575-83.

30. DSouza AV, Lin H, Henderson ER, et al. Review of fluorescence guided surgery systems: identification of key performance capabilities beyond indocyanine green imaging. J Biomed Opt 2016;21:80901.

31. Robinson BL, Donohue JH, Gunes S, et al. Selective Operative Cholangiography: Appropriate Management for Laparoscopic Cholecystectomy. Arch Surg 1995;130:625-30; discussion 630-1.

32. Flum DR. Intraoperative Cholangiography and Risk of Common Bile Duct Injury During Cholecystectomy. JAMA 2003;289:1639.

33. Ishizawa T, Tamura S, Masuda K, et al. Intraoperative Fluorescent Cholangiography Using Indocyanine Green: A Biliary Road Map for Safe Surgery. J Am Coll Surg 2009;208:e1-4.

34. Ishizawa T, Bandai Y, Ijichi M, et al. Fluorescent cholangiography illuminating the biliary tree during laparoscopic cholecystectomy. Br J Surg 2010;97:1369-77.

35. Mitsuhashi N, Kimura F, Shimizu H, et al. Usefulness of intraoperative fluorescence imaging to evaluate local anatomy in hepatobiliary surgery. J Hepatobiliary Pancreat Surg 2008;15:508-14.

36. Aoki T, Murakami M, Yasuda D, et al. Intraoperative fluorescent imaging using indocyanine green for liver mapping and cholangiography. J Hepatobiliary Pancreat Sci 2010;17:590-4.

37. Tagaya N, Shimoda M, Kato M, et al. Intraoperative exploration of biliary anatomy using fluorescence imaging of indocyanine green in experimental and clinical cholecystectomies. J Hepatobiliary Pancreat Sci 2010;17:595-600.

38. Ishizawa T, Kaneko J, Inoue Y, et al. Application of fluorescent cholangiography to single-incision laparoscopic cholecystectomy. Surg Endosc 2011;25:2631-6.

39. Buchs NC, Hagen ME, Pugin F, et al. Intra-operative fluorescent cholangiography using indocyanin green during robotic single site cholecystectomy. Int J Med Robot 2012;8:436-40.

40. Kaneko J, Ishizawa T, Masuda K, et al. Indocyanine green reinjection technique for use in fluorescent angiography concomitant with cholangiography during laparoscopic cholecystectomy. Surg Laparosc Endosc Percutan Tech 2012;22:341-4.

41. Buchs NC, Pugin F, Azagury DE, et al. Real-time near-infrared fluorescent cholangiography could shorten operative time during robotic single-site cholecystectomy. Surg Endosc 2013;27:3897-901.

42. Schols RM, Bouvy ND, Masclee AAM, et al. Fluorescence cholangiography during laparoscopic cholecystectomy: a feasibility study on early biliary tract delineation. Surg Endosc 2013;27:1530-6.

43. Schols RM, Bouvy ND, van Dam RM, et al. Combined vascular and biliary fluorescence imaging in laparoscopic cholecystectomy. Surg Endosc 2013;27:4511-7.

44. Spinoglio G, Priora F, Bianchi PP, et al. Real-time near-infrared (NIR) fluorescent cholangiography in single-site robotic cholecystectomy (SSRC): a single-institutional prospective study. Surg Endosc 2013;27:2156-62.

45. Verbeek FPR, Schaafsma BE, Tummers QRJG, et al. Optimization of near-infrared fluorescence cholangiography for open and laparoscopic surgery. Surg Endosc 2014;28:1076-82.

46. Prevot F, Rebibo L, Cosse C, et al. Effectiveness of intraoperative cholangiography using indocyanine green (versus contrast fluid) for the correct assessment

of extrahepatic bile ducts during day-case laparoscopic cholecystectomy. J. Gastrointest Surg 2014;18:1462-8.

47. Daskalaki D, Fernandes E, Wang X, et al. Indocyanine green (ICG) fluorescent cholangiography during robotic cholecystectomy: results of 184 consecutive cases in a single institution. Surg Innov 2014;21:615-21.

48. Larsen SS, Schulze S, Bisgaard T. Non-radiographic intraoperative fluorescent cholangiography is feasible. Dan Med J 2014;61:A4891.

49. Boni L, David G, Mangano A, et al. Clinical applications of indocyanine green (ICG) enhanced fluorescence in laparoscopic surgery. Surg Endosc 2015;29:2046-55.

50. Dip FD, Asbun D, Rosales-Velderrain A, et al. Cost analysis and effectiveness comparing the routine use of intraoperative fluorescent cholangiography with fluoroscopic cholangiogram in patients undergoing laparoscopic cholecystectomy. Surg Endosc 2014;28:1838-43.

51. Osayi SN, Wendling MR, Drosdeck JM, et al. Near-infrared fluorescent cholangiography facilitates identification of biliary anatomy during laparoscopic cholecystectomy. Surg Endosc 2015;29:368-75.

52. Dip F, Roy M, Lo Menzo E, et al. Routine use of fluorescent incisionless cholangiography as a new imaging modality during laparoscopic cholecystectomy. Surg Endosc 2015;29:1621-6.

53. van Dam DA, Ankersmit M, van de Ven P, et al. Comparing Near-Infrared Imaging with Indocyanine Green to Conventional Imaging During Laparoscopic Cholecystectomy: A Prospective Crossover Study. J Laparoendosc Adv Surg Tech A 2015;25:486-92.

54. Kono Y, Ishizawa T, Tani K, et al. Techniques of Fluorescence Cholangiography During Laparoscopic Cholecystectomy for Better Delineation of the Bile Duct Anatomy. Medicine (Baltimore) 2015;94:e1005.

55. Dip F, Nguyen D, Montorfano L, et al. Accuracy of Near Infrared-Guided Surgery in Morbidly Obese Subjects Undergoing Laparoscopic Cholecystectomy. Obes Surg 2016;26:525-30.

56. Zroback C, Chow G, Meneghetti A, et al. Fluorescent cholangiography in laparoscopic cholecystectomy: the initial Canadian experience. Am J Surg 2016;211:933-7.

57. Zarrinpar A, Dutson EP, Mobley C, et al. Intraoperative Laparoscopic Near-Infrared Fluorescence Cholangiography to Facilitate Anatomical Identification: When to Give Indocyanine Green and How Much. Surg Innov 2016;23:360-5.

58. Igami T, Nojiri M, Shinohara K, et al. Clinical value and pitfalls of fluorescent cholangiography during single-incision laparoscopic cholecystectomy. Surg Today 2016;46:1443-50.

59. Boogerd LSF, Handgraaf HJM, Lam HD, et al. Laparoscopic detection and resection of occult liver tumors of multiple cancer types using real-time near-infrared fluorescence guidance. Surg Endosc 2017;31:952-61.

60. Graves C, Ely S, Idowu O, et al. Direct Gallbladder Indocyanine Green Injection Fluorescence Cholangiography During Laparoscopic Cholecystectomy. J Laparoendosc Adv Surg Tech A 2017;27:1069-73.

61. Maker AV, Kunda N. A Technique to Define Extrahepatic Biliary Anatomy Using Robotic Near-Infrared Fluorescent Cholangiography. J Gastrointest Surg 2017;21:1961-2.

62. Liu YY, Liao CH, Diana M, et al. Near-infrared cholecystocholangiography with direct intragallbladder indocyanine green injection: preliminary clinical results. Surg Endosc 2018;32:1506-14.

63. Hiwatashi K, Okumura H, Setoyama T, et al. Evaluation of laparoscopic cholecystectomy using indocyanine green cholangiography including cholecystitis: A retrospective study. Medicine (Baltimore) 2018;97:e11654.

64. Yoshiya S, Minagawa R, Kamo K, et al. Usability of Intraoperative Fluorescence Imaging with Indocyanine Green During Laparoscopic Cholecystectomy After Percutaneous Transhepatic Gallbladder Drainage. World J Surg 2019;43:127-33.

65. Ambe PC, Plambeck J, Fernandez-Jesberg V, et al. The role of indocyanine green fluoroscopy for intraoperative bile duct visualization during laparoscopic cholecystectomy: an observational cohort study in 70 patients. Patient Saf Surg 2019;13:2.

66. Kaibori M, Ishizaki M, Matsui K, et al. Intraoperative indocyanine green fluorescent imaging for prevention of bile leakage after hepatic resection. Surgery 2011;150:91-8.

67. Sakaguchi T, Suzuki A, Unno N, et al. Bile leak test by indocyanine green fluorescence images after hepatectomy. Am J Surg 2010;200:e19-23.

68. Bismuth H, Eshkenazy R, Arish A. Milestones in the evolution of hepatic surgery. Rambam Maimonides Med J 2011;2:e0021.

69. Makuuchi M, Imamura H, Sugawara Y, et al. Progress in surgical treatment of hepatocellular carcinoma. Oncology 2002;62 Suppl 1:74-81.

70. Aoki T, Yasuda D, Shimizu Y, et al. Image-Guided Liver Mapping Using Fluorescence Navigation System with Indocyanine Green for Anatomical Hepatic Resection.

World J Surg 2008;32:1763-7.
71. Inoue Y, Arita J, Sakamoto T, et al. Anatomical Liver
Resections Guided by 3-Dimensional Parenchymal
Staining Using Fusion Indocyanine Green Fluorescence
Imaging. Ann Surg 2015;262:105-11.
72. Gotoh K, Yamada T, Ishikawa O, et al. A novel image-
guided surgery of hepatocellular carcinoma by indocyanine
green fluorescence imaging navigation. J Surg Oncol
2009;100:75-9.
73. Ishizawa T, Fukushima N, Shibahara J, et al. Real-time
identification of liver cancers by using indocyanine green
fluorescent imaging. Cancer 2009;115:2491-504.
74. Uchiyama K, Ueno M, Ozawa S, et al. Combined use of
contrast-enhanced intraoperative ultrasonography and
a fluorescence navigation system for identifying hepatic
metastases. World J Surg 2010;34:2953-9.
75. Uchiyama K, Ueno M, Ozawa S, et al. Combined
intraoperative use of contrast-enhanced ultrasonography
imaging using a sonazoid and fluorescence navigation
system with indocyanine green during anatomical
hepatectomy. Langenbecks Arch Surg 2011;396:1101-7.
76. Ishizuka M, Kubota K, Kita J, et al. Intraoperative
observation using a fluorescence imaging instrument
during hepatic resection for liver metastasis from
colorectal cancer. Hepatogastroenterology 2012;59:90-2.
77. Peloso A, Franchi E, Canepa MC, et al. Combined use
of intraoperative ultrasound and indocyanine green
fluorescence imaging to detect liver metastases from
colorectal cancer. HPB 2013;15:928-34.
78. Tanaka T, Takatsuki M, Hidaka M, et al. Is a fluorescence
navigation system with indocyanine green effective enough
to detect liver malignancies? J Hepatobiliary Pancreat Sci
2014;21:199-204.
79. Kudo H, Ishizawa T, Tani K, et al. Visualization of
subcapsular hepatic malignancy by indocyanine-green
fluorescence imaging during laparoscopic hepatectomy.
Surg Endosc 2014;28:2504-8.
80. Sakoda M, Ueno S, Iino S, et al. Anatomical laparoscopic
hepatectomy for hepatocellular carcinoma using
indocyanine green fluorescence imaging. J Laparoendosc
Adv Surg Tech A 2014;24:878-82.
81. Tummers QRJG, Verbeek FPR, Prevoo HAJM, et al. First
experience on laparoscopic near-infrared fluorescence
imaging of hepatic uveal melanoma metastases using
indocyanine green. Surg Innov 2015;22:20-5.
82. Yamamichi T, Oue T, Yonekura T, et al. Clinical
application of indocyanine green (ICG) fluorescent
imaging of hepatoblastoma. J Pediatr Surg 2015;50:833-6.
83. Barabino G, Porcheron J, Cottier M, et al. Improving
Surgical Resection of Metastatic Liver Tumors With Near-
Infrared Optical-Guided Fluorescence Imaging. Surg
Innov 2016;23:354-9.
84. Kaibori M, Matsui K, Ishizaki M, et al. Intraoperative
Detection of Superficial Liver Tumors by Fluorescence
Imaging Using Indocyanine Green and 5-aminolevulinic
Acid. Anticancer Res 2016;36:1841-9.
85. Takahashi H, Zaidi N, Berber E. An initial report on
the intraoperative use of indocyanine green fluorescence
imaging in the surgical management of liver tumorss. J
Surg Oncol 2016;114:625-9.
86. Zhang YM, Shi R, Hou JC, et al. Liver tumor boundaries
identified intraoperatively using real-time indocyanine
green fluorescence imaging. J Cancer Res Clin Oncol
2017;143:51-8.
87. Kawaguchi Y, Nomura Y, Nagai M, et al. Liver transection
using indocyanine green fluorescence imaging and hepatic
vein clamping. Br J Surg 2017;104:898-906.
88. Terasawa M, Ishizawa T, Mise Y, et al. Applications of
fusion-fluorescence imaging using indocyanine green in
laparoscopic hepatectomy. Surg Endosc 2017;31:5111-8.
89. Narasaki H, Noji T, Wada H, et al. Intraoperative Real-
Time Assessment of Liver Function with Near-Infrared
Fluorescence Imaging. Eur Surg Res 2017;58:235-45.
90. Kobayashi Y, Kawaguchi Y, Kobayashi K, et al. Portal
vein territory identification using indocyanine green
fluorescence imaging: Technical details and short-term
outcomes. J Surg Oncol 2017;116:921-31.
91. Lieto E, Galizia G, Cardella F, et al. Indocyanine Green
Fluorescence Imaging-Guided Surgery in Primary and
Metastatic Liver Tumors. Surg Innov 2018;25:62-8.
92. Nanashima A, Tominaga T, Sumida Y, et al. Indocyanine
green identification for tumor infiltration or metastasis
originating from hepatocellular carcinoma. Int J Surg Case
Rep 2018;46:56-61.
93. Cheung TT, Ma KW, She WH, et al. Pure laparoscopic
hepatectomy with augmented reality-assisted indocyanine
green fluorescence versus open hepatectomy for
hepatocellular carcinoma with liver cirrhosis: A
propensity analysis at a single center. Asian J Endosc Surg
2018;11:104-11.
94. Peyrat P, Blanc E, Guillermet S, et al. HEPATOFLUO:
A prospective monocentric study assessing the benefits of
indocyanine green (ICG) fluorescence for hepatic surgery.
J Surg Oncol 2018;117:922-7.
95. Nomi T, Hokuto D, Yoshikawa T, et al. A Novel
Navigation for Laparoscopic Anatomic Liver Resection

Using Indocyanine Green Fluorescence. Ann Surg Oncol 2018;25:3982.

96. Chiba N, Shimazu M, Ochiai S, et al. Resection of Hepatic Lesions Perfused by the Cholecystic Vein Using Indocyanine Green Navigation in Patients with cT2 Gallbladder Cancer. World J Surg 2019;43:608-14.

97. Alfano MS, Molfino S, Benedicenti S, et al. Intraoperative ICG-based imaging of liver neoplasms: a simple yet powerful tool. Preliminary results. Surg Endosc 2019;33:126-34.

98. He P, Huang T, Fang C, et al. Identification of extrahepatic metastasis of hepatocellular carcinoma using indocyanine green fluorescence imaging. Photodiagnosis Photodyn Ther 2019;25:417-20.

99. Urade T, Sawa H, Iwatani Y, et al. Laparoscopic anatomical liver resection using indocyanine green fluorescence imaging. Asian J Surg 2020;43:362-8.

100. Souzaki R, Kawakubo N, Matsuura T, et al. Navigation surgery using indocyanine green fluorescent imaging for hepatoblastoma patients. Pediatr Surg Int 2019;35:551-7.

101. Yoshioka M, Taniai N, Kawano Y, et al. Laparoscopic repeat hepatectomy with indocyanine green fluorescence navigation: A case report. J Nippon Med Sch 2019;86:291-5.

102. Marino MV, Builes Ramirez S, Gomez Ruiz M. The Application of Indocyanine Green (ICG) Staining Technique During Robotic-Assisted Right Hepatectomy: with Video. J Gastrointest Surg 2019;23:2312-3.

103. Maeda H, Wu J, Sawa T, et al. Tumor vascular permeability and the EPR effect in macromolecular therapeutics: a review. J Control Release 2000;65:271-84.

104. Ishizawa T, Harada N, Muraoka A, et al. Scientific Basis and Clinical Application of ICG Fluorescence Imaging: Hepatobiliary Canc er~!2009-10-02~!2009-12-23~!2010-05-26~! Open Surg Oncol J 2010;2:31-6.

105. Nakaseko Y, Ishizawa T, Saiura A. Fluorescence-guided surgery for liver tumors. J Surg Oncol 2018;118:324-31.

106. Handgraaf HJM, Boogerd LSF, Höppener DJ, et al. Long-term follow-up after near-infrared fluorescence-guided resection of colorectal liver metastases: A retrospective multicenter analysis. Eur J Surg Oncol 2017;43:1463-71.

107. Ishizawa T, Zuker NB, Kokudo N, et al. Positive and negative staining of hepatic segments by use of fluorescent imaging techniques during laparoscopic hepatectomy. Arch Surg Chic Ill 1960 2012;147:393-4.

108. Kawaguchi Y, Nagai M, Nomura Y, et al. Usefulness of indocyanine green-fluorescence imaging during

109. Mizuno S, Isaji S. Indocyanine green (ICG) fluorescence imaging-guided cholangiography for donor hepatectomy in living donor liver transplantation. Am J Transplant 2010;10:2725-6.

110. Mizuno S, Inoue H, Tanemura A, et al. Biliary complications in 108 consecutive recipients with duct-to-duct biliary reconstruction in living-donor liver transplantation. Transplant Proc 2014;46:850-5.

111. Kubota K, Kita J, Shimoda M, et al. Intraoperative assessment of reconstructed vessels in living-donor liver transplantation, using a novel fluorescence imaging technique. J Hepatobiliary Pancreat Surg 2006;13:100-4.

112. Figueroa R, Golse N, Alvarez FA, et al. Indocyanine green fluorescence imaging to evaluate graft perfusion during liver transplantation. HPB 2019;21:387-92.

113. Fu XY, Besterman JM, Monosov A, et al. Models of human metastatic colon cancer in nude mice orthotopically constructed by using histologically intact patient specimens. Proc Natl Acad Sci U S A 1991;88:9345-9.

114. Hoffman RM. Patient-derived orthotopic xenografts: better mimic of metastasis than subcutaneous xenografts. Nat Rev Cancer 2015;15:451-2.

115. Kubota T. Metastatic models of human cancer xenografted in the nude mouse: the importance of orthotopic transplantation. J Cell Biochem 1994;56:4-8.

116. Hoffman RM. Orthotopic metastatic mouse models for anticancer drug discovery and evaluation: a bridge to the clinic. Invest New Drugs 1999;17:343-59.

117. Yano S, Takehara K, Miwa S, et al. Improved Resection and Outcome of Colon-Cancer Liver Metastasis with Fluorescence-Guided Surgery Using In Situ GFP Labeling with a Telomerase-Dependent Adenovirus in an Orthotopic Mouse Model. PloS One 2016;11:e0148760.

118. Kishimoto H, Kojima T, Watanabe Y, et al. In vivo imaging of lymph node metastasis with telomerase-specific replication-selective adenovirus. Nat Med 2006;12:1213-9.

119. Hiroshima Y, Lwin TM, Murakami T, et al. Effective fluorescence-guided surgery of liver metastasis using a fluorescent anti-CEA antibody. J Surg Oncol 2016;114:951-8.

120. Gutowski M, Framery B, Boonstra MC, et al. SGM-101: An innovative near-infrared dye-antibody conjugate that targets CEA for fluorescence-guided surgery. Surg Oncol 2017;26:153-62.

121. Framery B, Gutowski M, Dumas K, et al. Toxicity and pharmacokinetic profile of SGM-101, a fluorescent anti-

CEA chimeric antibody for fluorescence imaging of tumors in patients. Toxicol Rep 2019;6:409-15.

122. Hoogstins CES, Boogerd LSF, Sibinga Mulder BG, et al. Image-Guided Surgery in Patients with Pancreatic Cancer: First Results of a Clinical Trial Using SGM-101, a Novel Carcinoembryonic Antigen-Targeting, Near-Infrared Fluorescent Agent. Ann Surg Oncol 2018;25:3350-7.

123. Hoogstins CES, Tummers QRJG, Gaarenstroom KN, et al. A Novel Tumor-Specific Agent for Intraoperative Near-Infrared Fluorescence Imaging: A Translational Study in Healthy Volunteers and Patients with Ovarian Cancer. Clin Cancer Res 2016;22:2929-38.

124. Rosenthal EL, Warram JM, de Boer E, et al. Successful Translation of Fluorescence Navigation During Oncologic Surgery: A Consensus Report. J Nucl Med 2016;57:144-50.

125. Tummers WS, Miller SE, Teraphongphom NT, et al. Detection of visually occult metastatic lymph nodes using molecularly targeted fluorescent imaging during surgical resection of pancreatic cancer. HPB (Oxford) 2019;21:883-90.

126. Tummers WS, Miller SE, Teraphongphom NT, et al. Intraoperative Pancreatic Cancer Detection using Tumor-Specific Multimodality Molecular Imaging. Ann Surg Oncol 2018;25:1880-8.